

## TOPICS ON WIND TURBINE AERODYNAMIC DESIGN

**Francisco Leme Galvão (B. S. & M. S.); urupema@directnet.com.br**  
Instituto Nacional de Pesquisas Espaciais (retired); São José dos Campos, SP, Brasil

**Abstract.** *This paper presents some topics related to wind turbine aerodynamic design:*

- *Power output of twin tandem rotors wind turbines, having two and three blades, estimated using classical momentum theory, and showing the possible power generation gains in comparison with usual single rotor wind turbines of the same diameter.*
- *Non planar, and twin tandem rotors configuration design.*
- *Single rotor aerodynamics, power coefficients, and blade shape computations, using a blade element momentum theory (BEM), modified in order to take into account finite wing aerodynamic theory concepts, applied to single, two, and three bladed rotors.*
- *Airfoil shapes for wind turbine blades tip, center, and root sections, designed using an author's simplified method, and having a high  $L^{1.5} / D$ , that is shown to be a key airfoil parameter for wind turbine performance.*

**Keywords:** *Wind turbine, Aerodynamic design, Airfoil, Rotor blade.*

### 1. TWIN ROTORS

The simpler approach usually used to analyze the wind energy extraction by a wind turbine is to consider it equivalent to a simple disk or “actuator disk”, a concept initially developed for propellers, that has also been applied to fans, helicopter rotors, etc., which main objectives are to provide and maximize axial forces and traction.

When applied to wind turbines the results are similar, with opposed sense.

From the continuity of the air flow, the comparison of the air axial momentum upstream and downstream of the disk, and application of the Bernoulli law ahead and after the rotor disk, it can be verified (Burton *et al.*, 2001) that the air velocity reduction “u”, caused by the wind turbine at the disk, is duplicated ( $2 \cdot u$ ) downstream, the same way the propeller air velocity increases, and the lifting wing downwash speeds are duplicated far behind them.

A wind turbine power coefficient is defined as:

$$C_p = 2 \cdot \text{Power} / \pi \cdot \rho \cdot W^3 \cdot R^2 \quad (1)$$

where  $\rho$  is the air density,  $W$  is the wind speed and  $R$  is the wind turbine rotor, or actuator disk radius.

Using  $u / W = a$ , the power coefficient can be written as:

$$C_p = 4 \cdot a \cdot (1 - a)^2 \quad (2)$$

The maximum  $C_p$  value can then be shown to be  $C_{p_{\max}} = 16 / 27 = 0,593$ , which corresponds to  $a = 1 / 3$ , and it is called the Betz limit, from Alfred Betz the German aerodynamicist who developed the momentum theory for propellers, and it has also been considered to limit the maximum power that could be extracted from the wind by a wind turbine.

However, additional considerations should be done about that, since it considers a single rotor, or disk.

The air velocity far behind a rotor will be  $W \cdot (1 - 2a)$ , and even for a rotor working at this maximum  $C_p$ , the wind speed behind it will be then at least  $W / 3$ .

The power being proportional to the cube of the wind speed, a second rotor with the same diameter, placed concentrically downwind of it, could then extract an additional power at least equal to  $(1/3)^3$  of that of the first rotor, and the total  $C_p$  for both rotors, referred to a single rotor area, will be then:  $C_p (\text{total}) \geq 0,593 \cdot (1 + 1/27) = 0,615$

By reducing the first rotor  $C_p$  the wind speed left for the second will be increased, and a new maximum theoretical  $C_p$  for twin tandem rotors with the same diameter can then be found, and it will correspond to a first rotor operating with  $C_p = 0,512$ , that is with  $a = 0,2$ , leaving behind it at least 60% of the wind speed for a second rotor with  $C_p = 0,593$ , so that for both rotors we have:  $C_p \geq 0,512 + 0,593 (0,6)^3 = 0,640$ , also 8% above the Betz limit!

Theoretically, for a sequence of rotors placed in tandem with diameters increasing by a factor  $1 / (1 - 2a)^{0,5}$ , the downwind speed will tend to zero, and the total  $C_p$  (always referred to the first rotor area) will tend to 1!

In “Tab. 1”, more realistic figures for the total  $C_p$  of four wind turbines, having tandem rotors of the same diameter, with two, and or three blades, are estimated assuming that  $C_p$  and “a” are related by “Eq. 2” with the inclusion in it of an efficiency factor  $\epsilon$ , in order to reproduce the typical  $C_p$  values for two and three bladed rotors given in “Fig. 1”.

The wind speed at the second rotor is conservatively assumed to be  $W \cdot (1 - 2a)$ .

The results show for the twin three bladed rotors combination, a  $C_p \geq 0,507$ , also at least 8% above 0,470, the maximum typical  $C_p$  of a single three bladed wind turbine.

Considering that each blade cost is about 7% of the total wind turbine cost (Burton *et al.*, 2001), this 8% power gain would correspond to a 21% initial cost increase, to be paid in the long run by the increased power output. Since a simple 4% increase in the wind turbine diameter would lead to the same power increase, the twin rotor turbine seems to present little advantage unless for cases where the diameter is limited by constructional, transport, or other constraints.

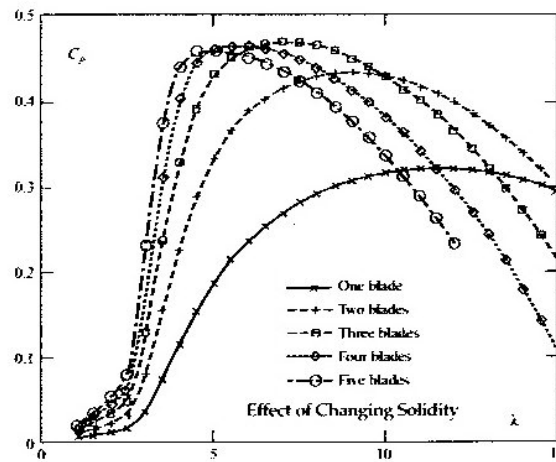


Figure 1 - Typical wind turbine Cp values (Burton *et al.*, 2001)

Table 1 – Estimated characteristics of four tandem rotors, with two and three blades.

		Rotors					2 Rotors in Tandem				
Rotor Blades		$\epsilon$	$a$	$C_p$	$V$	$C_p \cdot V^3$	Blades	$C_p$	Cost	Power	
1	Front	2	0,734	0,160	0,331	1,000	0,331	4	0,468	107,0%	99,6%
	Rear	2	0,734	0,333	0,435	0,680	0,137				
2	Rear	3	0,793	0,333	0,470	0,680	0,148	5	0,479	114,0%	102,0%
	Front	3	0,793	0,215	0,420	1,000	0,420				
3	Rear	2	0,734	0,333	0,435	0,570	0,081	5	0,501	114,0%	106,6%
	Front	2	0,734	0,160	0,331	1,000	0,331				
4	Rear	3	0,793	0,333	0,470	0,570	0,087	6	0,507	121,0%	107,9%
	Front	3	0,793	0,215	0,420	1,000	0,420				

$C_p = 4 \cdot \epsilon \cdot a \cdot (1 - a)^2$ , and  $V = 1 - 2 \cdot a$

The “Table 1” values however, do not take into account the eventual interference induced drag (see section 3) reduction effects due to gap increase, that could affect rotors, the same way in biplane wings the total induced drag is reduced by increasing the gap between the wings, as shown in “Fig. 2”, where the results obtained by the author using a vortex lattice program (Lamar, 1971), are compared with the Munk’s k factor (Warner, 1936).

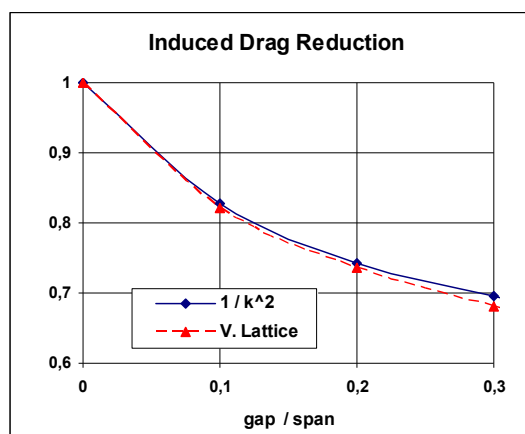


Figure 2 – Biplane wing induced drag reduction factors.

It is reasonable to expect some similar interference reduction effect in tandem rotors, as function of increasing values of the gap between them, but since to increase the gap also means to reduce the wind at the second rotor, an optimal gap value should exist, but its determination will need the correct knowledge of both, the interference effect, and the wake speed decrease with distance.

The previous paragraph simple analysis, and “Tab. 1” computations, also do not also take into account the effects of

the tangential speeds (see section 2), or the wake rotation, induced by the first rotor, that in the case of rotors rotating in opposing senses, will result in an increase of the wind power available to the second rotor.

The counter rotating rotor scheme could also reduce the weight of the gear box drive train, if the electric generator rotor is geared to one wind turbine rotor, and its stator to the other.

Tests with a twin two blade rotors wind turbine, with 1,4 m diameter (Munkund, 2005), showed in comparison to the single two bladed rotor turbine, a 40% increase in the power absorbed, and a much lower vibration level, so it seems that the twin rotor wind turbine deserves much more theoretical, and experimental investigation.

Twin tandem rotors configurations will also be better suited to the use of non planar rotors with blades having continuous or discrete dihedral angles along the radius, or with tip “winglets”.

According to Cone (Cone, 1962) the induced drag of non planar lifting surfaces can be even lower than that of planar elliptical surfaces, considered before to have the least induced drag of all wing shapes having the same span and area.

In airplane design, the trend started with gliders (soaring birds mimicking) to use “winglets” or pronounced dihedral wing tips like those of the new Boeing 787, show that beyond lateral stability, induced drag reductions are seek.

Non planar rotors with coning angles, “winglets”, etc. are already used in some wind turbines for many reasons, inclusive noise reductions, etc, but since in most of them the supporting tower is mounted at rotor leeside, to avoid collision with it, angles and bends must be done on the opposed direction, otherwise a large unbalanced rotor arm would be needed. As a side effect, the blade bending moments are increased due to centrifugal inertia forces.

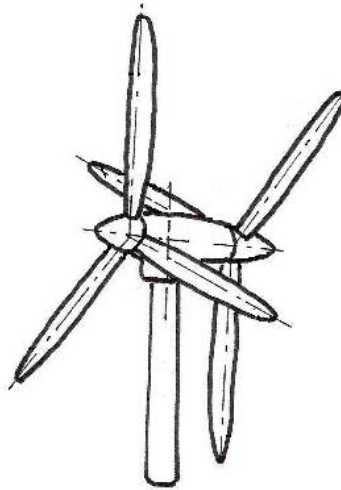


Figure 3 – A twin tandem rotor wind turbine configuration.

A twin rotor configuration with a gap between the rotors, and with the supporting tower placed between them as shown in “Fig. 3”, would otherwise help to obtain a better balanced design when using non planar blades with dihedral angles in the blade suction side direction, what besides reducing blade induced drag will also reduce the blade bending moments, by opposing the effects of the centrifugal inertia forces to the aerodynamic ones.

It could also help the turbine assembly windward orientation by providing more favorable yawing moments.

## 2. POWER, TORQUE, AND INDUCED SPEEDS

A basic physical principle (Newtonian) is that for any force exerted by a fluid over a solid surface shall correspond to fluid velocities induced in the opposed sense, and proportional to this force, and so the thrust or drag of rotating aerodynamic devices being axial forces, shall correspond to induced axial air velocities, while shaft torque and power, resulting from tangential forces, shall correspond to induced tangential velocities.

In the design of propellers, helicopter rotors, and fans, the objective is to maximize their axial force (thrust), and so it is the axial component of the air velocities induced by them, that must be maximized and optimized.

In the case of wind turbines, however, the objective is to extract the maximum useful shaft power from the wind, and so it is the tangential component of the induced air velocities that need to be considered, instead.

The optimum induced air speed distribution that will maximize the torque and power could be found by using a vortex surface model, as usually done for airplane wings, but unlike for wings, which have a nearly plane slipstream of trailing vortices, and for which even a simple vortex line theory can already provide a rather accurate solution, the wind turbine helical surface slipstream makes this a quite complex problem, better treated by CFD programs.

For planar wings, given the span and the total lift, the smallest induced drag is found for elliptical untwisted wings, which result in elliptical loading distributions, and constant downwash induced velocities as shown in “ Fig. 4”.

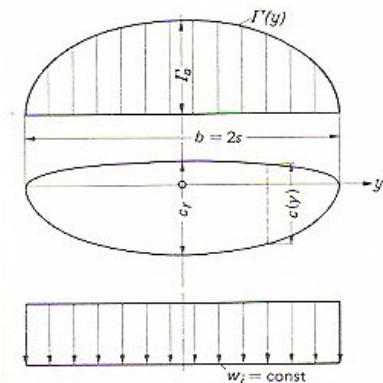


Figure 3-11 Elliptic circulation distribution with the corresponding elliptic wing planform and the constant induced downwash velocity over the wing span.

Figure 4 - Vortex line results (Schlichting *et al.*, 1969)

For wind turbines, it should be also expected that in order to minimize the induced drag, the total induced speeds should be kept constant, which means that either both normal and tangential speeds are kept constant, or in the case the tangential speeds should increase from blade tip towards root (Burton *et al.*, 2001), the normal speeds should accordingly decrease in order to keep the total induced speed constant.

**3. A BLADE ELEMENT MOMENTUM (BEM) THEORY**

Considering the complexity of the vortex approach we can use the simpler one, known as blade element momentum theory, but adapted in order to explicitly determine the induced component of the blade element drag.

The velocity of a blade element situated at a distance *r* of the rotor axle, relative to the far upstream incoming air, or wind velocity *W*, considering the blade rotation  $\Omega$  is:

$$V = (\Omega^2 \cdot r^2 + W^2)^{0.5} \tag{3}$$

The usual BEM approach (Burton *et al.*, 2001) uses the relative air velocity vector at the rotor, *V'* (see “Fig. 5”) as reference, but using *V* seems to be more consistent with finite wing aerodynamic theories, and airfoil wind tunnel tests.

The component normal to *V*, of the force acting on a blade element with dimensions *c*, and *dr*, is by definition its lift force, and with  $\rho$  being the air density, and  $C_L$  the lift force non dimensional coefficient, it can be written as:

$$\Delta L = C_L \cdot \rho / 2 \cdot V^2 \cdot c \cdot dr \tag{4}$$

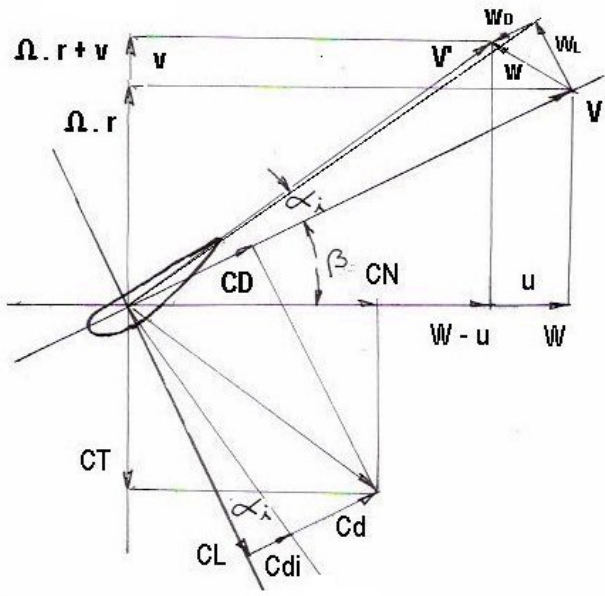


Figure 5 - Airspeeds and force coefficients in the blade element

The lift force must be also equal to the momentum variation in the direction normal to  $V$  of the deflected air, which we may consider to be the air flowing through a rectangular tube having a base  $dr$  and an height  $H$ .

If  $w_L$  is the induced velocity normal to  $V$  at the blade element, according to the finite wing theory (Schlichting *et al.*, 1969), it will be equal to  $2w_L$  far downstream, and applying the force momentum change equivalence we can write:

$$\Delta L = \rho \cdot H \cdot dr \cdot V' \cdot 2w_L \quad (5)$$

The induced drag is the component in the  $V$  direction of the same pressure forces that create the lift and that result from the deflection of the air of an “induced angle”  $w_L / V$ , and from “Fig. 5” we can write:

$$Cd_i / C_L = w_L / V \quad (6)$$

With  $w_L$  obtained from equations 4 and 5, and assuming  $V^2 / V' \approx V$ , we have:

$$Cd_i = C_L^2 \cdot c / 4 \cdot H \quad (7)$$

This is similar to the well known expression  $Cd_i = C_L^2 \cdot S / \pi \cdot b^2$ , applicable to the induced drag of an elliptical wing with span  $b$  and area  $S$ , and that can also be deduced by considering that it deflects the air inside a tube having a circular cross section with diameter  $b$ , with a uniform speed or “downwash”.

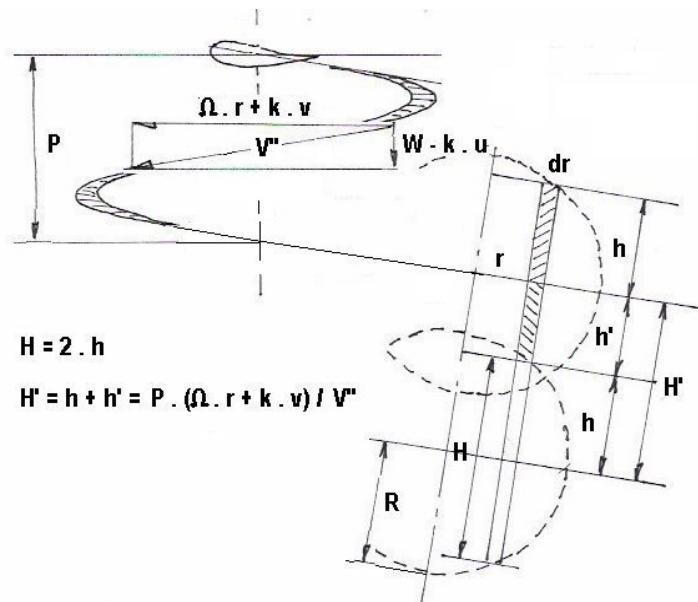


Figure 6 – Blade wake and downstream deflected air cross section.

Using the same reasoning we may suppose that the air deflected by a rotor blade with radius  $R$  would be inside a tube with diameter  $R$ , and the air deflected by a blade element inside a rectangular tube with base  $dr$  and height  $H$ , with:

$$H = 2 \cdot R \cdot (r / R \cdot (1 - r / R))^{0.5} \quad (8)$$

However due to the blade rotation  $\Omega$ , as shown in “Fig. 6”, the tube height shall be limited to the distance  $H'$  due to the air already deflected by a previous passing blade, or for a single blade rotor, by the blade in its previous passage.

The normal and tangential induced speeds varying from  $u$  and  $v$  up to  $2u$  and  $2v$ , their mean value along a circular path with length  $2\pi \cdot r / N$  downwind of the blade element, can be written as  $k \cdot u$ , and  $k \cdot v$ , with  $1 < k < 1.5$ .

For a rotor with  $N$  blades, the time for a blade to encounter a previously deflected air tube is  $2\pi / N \cdot \Omega$ , and with the mean air tube downwind (axial) speed being  $W - k \cdot u$ , the distance  $P$  between two consecutive tubes centers will be:

$$P = (2\pi / \Omega \cdot N) \cdot (W - k \cdot u) \quad (9)$$

That projected in the direction normal to the mean deflected airspeed  $P$  gives:

$$H' = (2\pi / \Omega \cdot N) \cdot (1 / (W - k \cdot u)^2 + 1 / (\Omega \cdot r + k \cdot v)^2)^{0.5} \quad (10)$$

From “Fig 5”, and from momentum equations:

$$u^2 + v^2 = w_L^2 + w_D^2 \quad (11)$$

$$u / v = C_N / C_T \quad (12)$$

$$w_L / w_D = C_L / C_D \quad (13)$$

$$u = w_L \cdot [(1 + C_D^2 / C_L^2) / (1 + C_T^2 / C_N^2)]^{0.5} \quad (14)$$

$$v = w_L \cdot [(1 + C_D^2 / C_L^2) / (1 + C_N^2 / C_T^2)]^{0.5} \quad (15)$$

For a given blade element  $C_L$  and  $c$ , the induced speeds, and  $H'$  can be iteratively computed together with  $C_{di}$ , and then the blade element total drag  $C_D$  determined by the sum of the induced drag and the blade element airfoil drag  $C_d$ , that can be obtained from 2 D analysis, or from 2D wind tunnel tests.

$$C_D = C_d + C_{di} \quad (16)$$

Also from “Fig. 5”, the normal and the tangential force coefficients at the blade element are:

$$C_N = (C_L \cdot \Omega \cdot r + C_D \cdot W) / V \quad (17)$$

$$C_T = (C_L \cdot W - C_D \cdot \Omega \cdot r) / V \quad (18)$$

Finally the contribution of the blade element to the rotor power, and power coefficient are:

$$\Delta P = C_T \cdot \rho / 2 \cdot V^2 \cdot \Omega \cdot r \cdot c \cdot dr \quad (19)$$

$$\Delta C_p = (C_T / \pi) \cdot (V / W)^2 \cdot (\Omega \cdot r / W) \cdot (c / R) \cdot (dr / R) \quad (20)$$

The above equations and the  $C_d$  values of the NACA 64 618 smooth airfoil (Abbot & Doenhoff, 1958) for  $C_L = 1$ , were used in an iterative spreadsheet to compute a three bladed wind turbine, with,  $c / R = 0,462$  at  $r / R = 0,75$ , and the remaining  $c / R$  values computed in order to keep  $w$  constant (see last paragraph of section 2) along  $r$ .

The fourth iteration numerical computation results, including the max  $C_p$ , are presented in “Tab. 2”, with the corresponding induced speeds  $u$ ,  $v$  and  $w$  presented in “Fig. 7”, and the resulting blade plan form given in “Fig. 8”.

Table 2 – Fourth iteration results for a 3 bladed wind turbine,  $C_p = 0,473$ , for  $\lambda = 7$ ,  $C_L = 1,0$ ,  $C_d = 0,006$ , and  $k = 1,2$ .

r / R	H' / R	H <sub>2</sub> / R	H / R	Ω r / W	V / W	ω <sub>L</sub> H / c	c / R	ω <sub>L</sub> / W	C <sub>D</sub>	C <sub>T</sub>	C <sub>N</sub>	v / W	u / W	w / W	d r / R	ΔC <sub>p</sub>
0,990	0,199	0,187	0,187	6,930	7,002	1,750	0,0353	0,330	0,053	0,090	0,9973	0,030	0,330	0,331	0,020	0,0067
0,960	0,392	0,187	0,187	6,720	6,794	1,698	0,0364	0,330	0,055	0,093	0,9971	0,031	0,329	0,331	0,040	0,0131
0,910	0,572	0,187	0,187	6,370	6,448	1,612	0,0383	0,330	0,057	0,099	0,9968	0,033	0,329	0,331	0,060	0,0187
0,840	0,733	0,187	0,187	5,880	5,964	1,491	0,0414	0,330	0,061	0,107	0,9961	0,035	0,329	0,331	0,080	0,0230
<b>0,750</b>	0,866	0,187	0,187	5,250	5,344	1,336	<b>0,0462</b>	0,330	0,068	0,121	0,995	0,040	0,329	0,331	0,100	<b>0,0256</b>
0,650	0,954	0,187	0,187	4,550	4,659	1,165	0,0529	0,330	0,077	0,140	0,9932	0,046	0,328	0,331	0,100	0,0222
0,550	0,995	0,186	0,186	3,850	3,978	0,994	0,0619	0,330	0,089	0,165	0,9902	0,055	0,327	0,331	0,100	0,0186
0,450	0,995	0,186	0,186	3,150	3,305	0,826	0,0742	0,330	0,106	0,202	0,9851	0,067	0,325	0,331	0,100	0,0149
0,350	0,954	0,185	0,185	2,450	2,646	0,662	0,0921	0,329	0,130	0,257	0,9751	0,085	0,321	0,332	0,100	0,0111
0,250	0,866	0,183	0,183	1,750	2,016	0,504	0,1193	0,328	0,169	0,350	0,9519	0,115	0,312	0,333	0,100	0,0071
0,160	0,733	0,179	0,179	1,120	1,501	0,375	0,1551	0,326	0,223	0,500	0,8945	0,163	0,291	0,334	0,080	0,0028
0,090	0,572	0,167	0,167	0,630	1,182	0,295	0,1831	0,323	0,279	0,697	0,7694	0,225	0,249	0,335	0,060	0,0006
0,040	0,392	0,144	0,144	0,280	1,038	0,260	0,1779	0,321	0,315	0,878	0,573	0,282	0,184	0,336	0,040	4E-05
0,010	0,199	0,115	0,115	0,070	1,002	0,251	0,1468	0,320	0,325	0,975	0,3945	0,312	0,126	0,337	0,020	3E-07
<b>N · Σ ΔC<sub>p</sub> =</b>																<b>0,473</b>

It is interesting to remark that the largest  $C_p$  contribution is given by the blade element at  $x / c = 0,75$ , and also the large blade root  $C_D$  values, in comparison to the airfoil  $C_d$ , showing the importance of the induced drag.

The same calculation procedure was applied for single and for two bladed rotors having approximately the same blade area, resulted in the plan forms shown in “Fig. 9”, and in  $C_p = 0,453$ , with  $\lambda = 9$ ,  $C_L = 1,05$ ,  $C_d = 0,008$ , and  $k = 1,3$ , for the two bladed rotor, and  $C_p = 0,424$ , with  $\lambda = 11,5$ ,  $C_L = 1,2$ ,  $C_d = 0,0115$ , and  $k = 1,4$  for the single blade rotor.

These computed  $C_p$  values are higher than those presented in “Fig. 1”, however if the “Fig. 8” blade plan form is used for the two bladed, and for the single blade rotor, the maximum computed  $C_p$  fall to: 0,438 for  $\lambda = 9$ , and 0,353 for  $\lambda = 11,5$  respectively. Also their computed  $C_p$  variation with  $\lambda$  is found to be more similar to that shown in “Fig. 1”.

Finally a more “practical” three bladed wind turbine was computed for a mean airfoil  $C_d = 0,0100$ , resulting in a  $C_p = 0,459$ , the blade plan form of “Fig. 10”, and the corresponding induced air velocities shown in “Fig 11”.

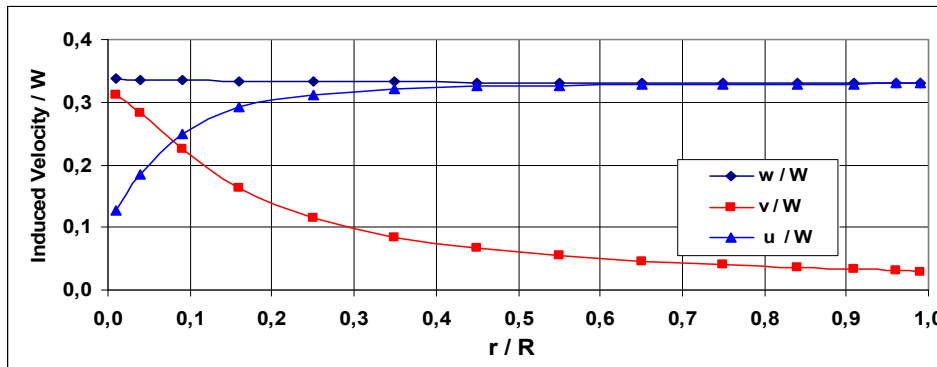


Figure 7 – Non dimensional induced velocities for the 3 bladed wind turbine.

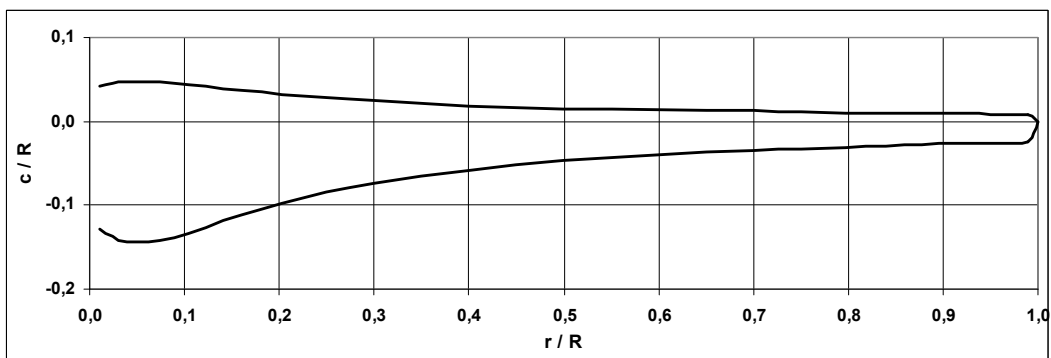


Figure 8 – Blade plan form of the three bladed wind turbine.

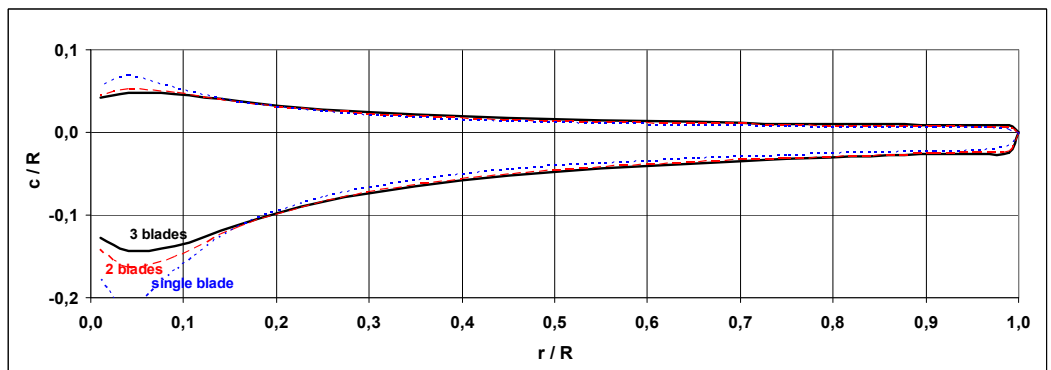


Figure 9 – Computed blade plan forms for one, two, and three bladed rotors ( $\lambda = 11,5, 9$  and  $7$  respectively).

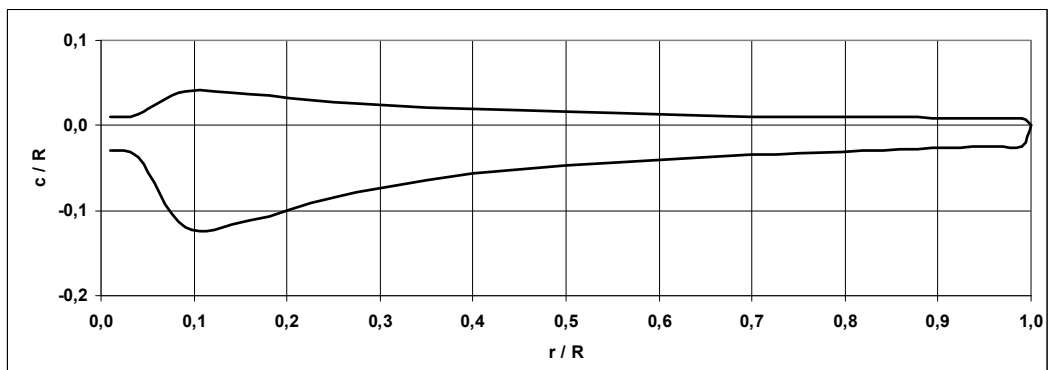


Figure 10 – “Practical” blade for a 3 bladed wind turbine,  $C_p = 0,459$  for  $\lambda = 7$ ,  $C_L = 1,0$ ,  $C_d = \mathbf{0,010}$ , and  $k = 1,2$ .

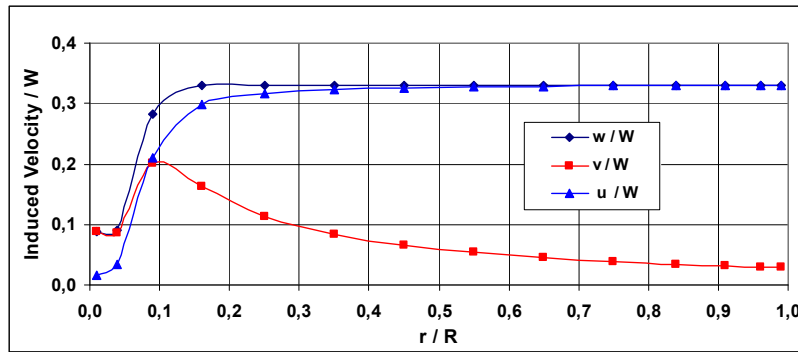


Figure 12 – Non dimensional induced velocities for the practical blade (3 bladed wind turbine).

#### 4. WIND TURBINE AIRFOILS

To verify the effects of the blade airfoil characteristics on a wind turbine performance, the “Table 2” computations were repeated for various  $C_L$  values, using the  $C_d$  of the NACA 64 618 airfoil, available both in clean and rough conditions for a Reynolds of 6 million (Abbot & Doenhoff, 1958), and the results are shown in “Table 3”.

Table 3 – Airfoil characteristics effects on wind turbine  $C_p$ .

CL	Clean Airfoil				Rough airfoil			
	Cd	CL / Cd	CL <sup>1.5</sup> /Cd	CP	Cd	CL / Cd	CL <sup>1.5</sup> /Cd	CP
<b>0,70</b>	0,0052	134,6	112,6	0,397	0,0122	57,4	48,0	0,373
<b>0,80</b>	0,0053	150,9	135,0	0,434	0,0133	60,2	53,8	0,407
<b>0,90</b>	0,0054	166,7	158,1	0,461	0,0148	<b>60,8</b>	57,7	0,429
<b>0,95</b>	0,0056	<b>169,6</b>	165,3	0,469	0,0157	60,5	59,0	0,434
<b>1,00</b>	0,0060	166,7	<b>166,7</b>	<b>0,473</b>	0,0169	59,2	<b>59,2</b>	<b>0,435</b>
<b>1,05</b>	0,0068	154,4	158,2	0,469	0,0185	56,8	58,2	0,428
<b>1,10</b>	0,0088	125,0	131,1	0,454	0,0210	52,4	54,9	0,411

It can be verified that for both, the smooth and the rough airfoil, the maximum wind turbine  $C_p$  values coincide with the airfoil maximum  $C_L^{1.5} / C_d$  ratio, and not with its maximum  $C_L / C_d$ .

This result is in a good agreement with airplane and glider performance analysis (Perkins, and Hage, 1965), for which the minimum required power for flight (and maximum climb) condition, is obtained for max  $C_L^{1.5} / C_d$ , while the maximum  $C_L / C_d$  corresponds to the maximum gliding flight condition.

In “Fig. 13”, “Fig. 14”, and “Fig. 15”, are presented three airfoils, designed using a simplified method (Galvão, 2005), with the objective to have high  $C_L^{1.5} / C_d$  values, and intended to be used for tip, middle, and root sections of wind turbine blades.

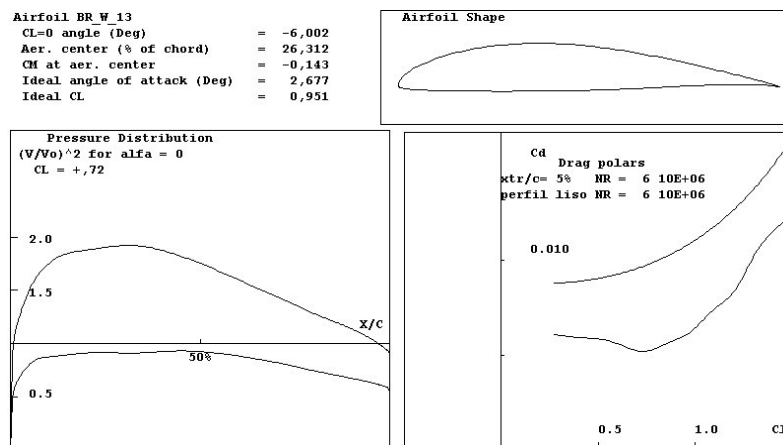


Figure 13 – Airfoil for a wind turbine blade tip.

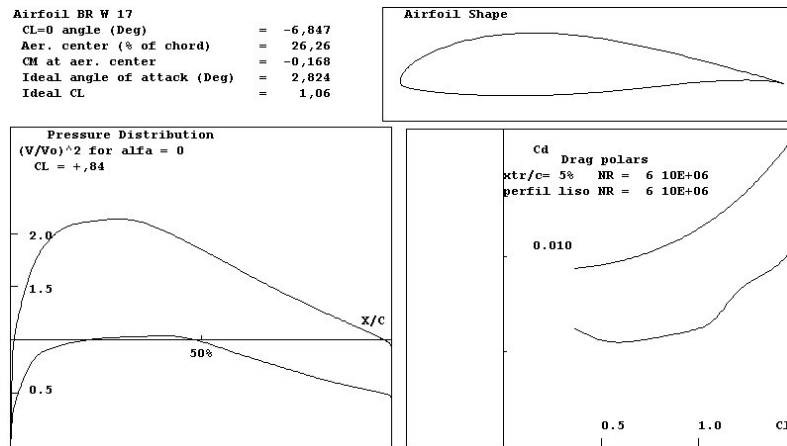


Figure 14 – Airfoil for a wind turbine blade middle section.

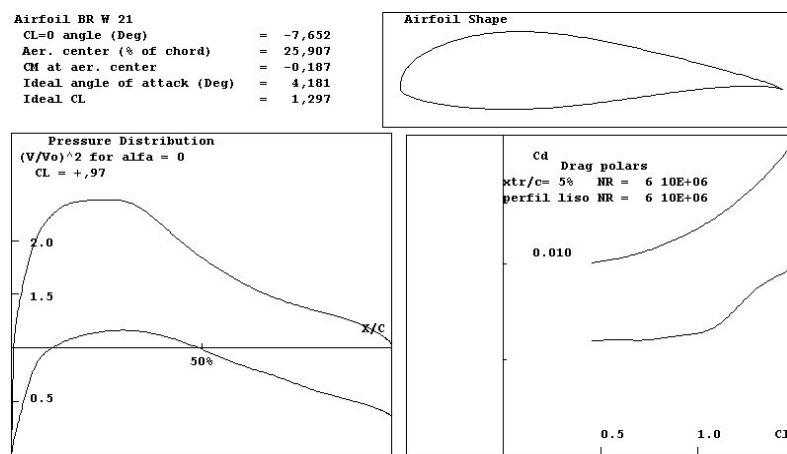


Figure 15 – Airfoil for a wind turbine blade root.

The computed  $C_L^{1,5} / C_d$  parameters for the three BRW airfoils are given in “Fig. 16” below.

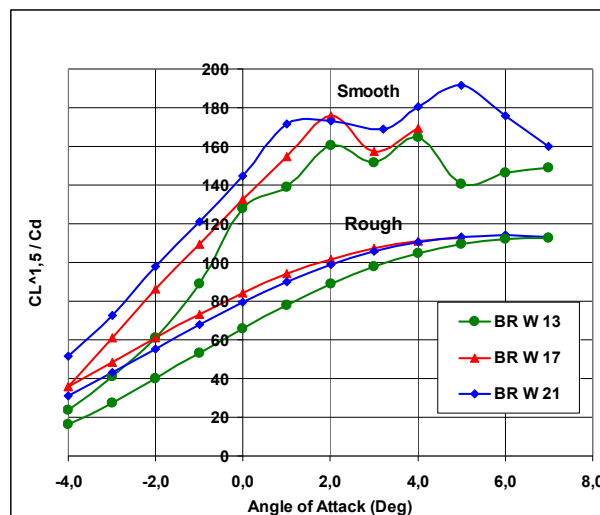


Figure 16 – Computed  $C_L^{1,5} / C_d$  for the BRW airfoils (NR = 6 millions).

- “Figure 17” in the next page makes a comparison between the BRW17, and the NACA 64 618 airfoil considering:
- The theoretical calculations done using the simplified analysis method, (Galvão, 2005), for a Reynolds Number of 6 millions, for both, rough and smooth airfoil conditions.
  - ITA/CTA Wind tunnel tests for both airfoils in rough condition and NR = 2,2 million (Cavallieri & Girardi, 2008).

The values computed from the NACA wind tunnel tests of the 64 618 airfoil, at a Reynolds Number of 6 millions (Abbot & Doenhoff, 1958) are also included in the figure.

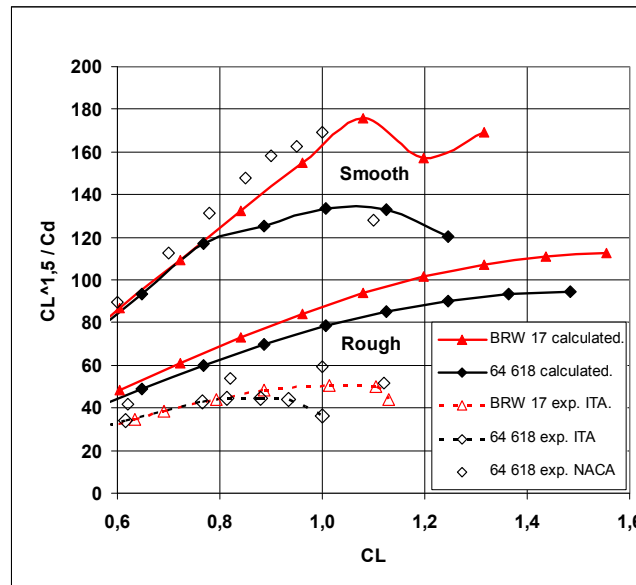


Figure 17 – Comparison between the BRW17, and the NACA 64 618 airfoil.

## 6. CONCLUSIONS

Double rotors in tandem configurations can be used to increase a wind turbine maximum power output, without the need to increase its diameter, and their performance, including with non planar rotors, deserves more deep theoretical and experimental investigation.

Finite wing theory concepts applied to blade element momentum theory, provide a simple tool for the design of wind turbine blades, and also show that the maximum wind turbine power for designs having constant total induced velocities along its radius is found for  $C_L$  values corresponding to the airfoil maximum  $C_L^{1.5} / C_d$  ratio.

Considering this criteria, the three BRW airfoils presented in this paper, seems to represent an adequate choice to be used for wind turbines blades.

## 7. REFERENCES

- Abbot, I. H. & Doenhoff, A. E.; "Theory of Wing Sections"; Dover Publications, New York, 1958 Ed.
- Burton, T.; Sharpe, D.; Jenkins, N.; Bossanyi, E.; "Wind Energy Handbook"; John Wiley & Sons, Chichester, England, 2001.
- Cavaliere, A. V. G. & Girardi, R. M.; "Ensaio do Perfil BRW17 no tunel de vento de ensino e pesquisa do ITA"; Relatório Técnico LPF-A-2008-3, ITA/CTA, São José dos Campos, dez. 2008.
- Cone, C. D.; "The theory of induced lift and minimum induced drag of non planar lifting systems"; NASA TR 139 NLRC, VA, USA, 1962
- Galvão, F. L.; "Wing Airfoil Simplified Design and Analysis"; SAE TP 2005-01-3974 E; SAE 2005.
- Lamar, J. E.; Margason, J. M.; "Vortex Lattice FORTRAN Program for Estimating Subsonic Aerodynamic Characteristics of Complete Plan forms"; NASA TN D 6142; NLRC; VA; Feb. 1971.
- Mukund, R. P.; "Wind and Solar Power Systems. Design Analysis and Operation"; Taylor & Francis, second Edition, 2005.
- Perkins, C. D.; Hage, R. E.; "Airplane Performance, Stability, and Control"; John Wiley & Sons, Inc.; 1965.
- Schlichting, H.; Truckenbodt, E.; Ramm, H. J. "Aerodynamics of the Airplane" Mac Graw Hill – 1979.
- Warner, E. P.; "Airplane Design - Performance"; Mac Graw Hill Book Co.; NY, 1936.

## 8. RESPONSIBILITY NOTICE

The author is the only responsible for the printed material included in this paper.